Expression of MeCP2 in postmitotic neurons rescues Rett syndrome in mice

Sandra Luikenhuis*†, Emanuela Giacometti*, Caroline F. Beard*, and Rudolf Jaenisch*†‡

*Whitehead Institute for Biomedical Research, †Massachusetts Institute of Technology, 9 Cambridge Center, Cambridge, MA 02142

Contributed by Rudolf Jaenisch, March 8, 2004

Mutations in *MECP2* are the cause of Rett syndrome (RTT) in humans, a neurodevelopmental disorder that affects mainly girls. MeCP2 is a protein that binds CpG dinucleotides and is thought to act as a global transcriptional repressor. It is highly expressed in neurons, but not in glia, of the postnatal brain. The timing of MeCP2 activation correlates with the maturation of the central nervous system, and recent reports suggest that MeCP2 may be involved in the formation of synaptic contacts and may function in activity-dependent neuronal gene expression. Deletion or targeted mutation of *Mecp2* in mice leads to a Rett-like phenotype. Selective mutation of *Mecp2* in postnatal neurons leads to a similar, although delayed, phenotype, suggesting that MeCP2 plays a role in postmitotic neurons. Here we test the hypothesis that the symptoms of RTT are exclusively caused by a neuronal MeCP2 deficiency by placing *Mecp2* expression under the control of a neuron-specific promoter. Expression of the *Mecp2* transgene in postmitotic neurons resulted in symptoms of severe motor dysfunction. Transgene expression in *Mecp2* mutant mice, however, rescued the RTT phenotype.

Rett syndrome (RTT), a neurodevelopmental disorder, is a leading cause of mental retardation in females with an estimated prevalence of 1 in 10,000–15,000 female births. RTT patients develop normally until 6–18 months of age, when they start to show symptoms including respiratory irregularities, progressive loss of motor skills, stereotypic hand movements, seizures, and features of autism. Examination of the brain reveals profound microencephaly due, at least in part, to smaller, more densely packed neurons. Other abnormalities include a reduction in dendritic arborization (1, 2). In ≈80% of cases, RTT is associated with mutations in the X-linked *MECP2* gene that is subject to inactivation when located on the inactive X chromosome (3). Therefore, heterozygous mutant females are mosaic for MeCP2 deficiency and show a wide range of phenotypes. Males, however, show a more severe phenotype, usually involving encephalopathy, motor abnormalities, and respiratory dysfunction. They rarely live beyond 2 years (2).

Mecp2 encodes a protein that binds specifically to methylated CpG dinucleotides and recruits chromatin remodeling complexes that contain the transcriptional repressor Sin3A and histone deacetylases 1 and 2 (4). In mouse, the protein localizes to highly methylated pericentromeric heterochromatin (5). Although MeCP2 is found in most tissues and cell types, highest expression levels are detected in the brain, where it is primarily present in neurons but not in glia (5–7). The timing of *Mecp2* expression correlates with the maturation of the CNS (5, 8), and recent reports suggest that MeCP2 may be involved in the formation of synaptic contacts (9). Although biochemical evidence suggests that MeCP2 acts as a global silencer, transcriptional profiling has failed to detect global changes in gene expression (10). A candidate approach has identified *BDNF*, a gene involved in neuronal survival, development, and plasticity, as a target for MeCP2 (11). These findings are consistent with MeCP2 playing a role in the maintenance and modulation of neuronal maturity. In particular, MeCP2 may function as a key regulator of activity-dependent neuronal gene expression.

Complete or partial deletion of *Mecp2* in mice leads to a neurological phenotype that is similar but less severe than human RTT (12, 13). Heterozygous females remain healthy into adulthood. In contrast, *Mecp2* mutant males appear normal and healthy at birth but begin to show a phenotype that resembles the human condition at 3–8 weeks of age, and die at 6–10 weeks of age. Mutant brains show a reduction in brain weight and neuronal cell size but no obvious structural defects or signs of neurodegeneration. Conditional mutation of *Mecp2* in the neural progenitor cells at embryonic day 12 results in a phenotype identical to that of the null mutation (12). Mutation of *Mecp2* in the postnatal neurons of restricted regions in the brain leads to a similar although delayed neuronal phenotype, suggesting that MeCP2 plays a role in postmitotic neurons (12). Here we test the hypothesis that the phenotype is exclusively caused by a neuronal MeCP2 deficiency by placing *Mecp2* expression under the control of a neuron-specific promoter. Overexpression of the *Mecp2* transgene in postmitotic neurons proved to be detrimental and led to symptoms of severe motor dysfunction. Transgene expression in *Mecp2* mutant mice, however, resulted in a rescue of the RTT phenotype.

Materials and Methods

Gene Targeting Construct. To introduce the *Mecp2* coding sequence as an in-frame fusion into exon 1 of the *tau* locus, we first cloned a 3.8-kb *Kpn*I/*Eco*RI fragment from pHV, which contains 14-kb of *tau* genomic sequence (kindly provided by K. Tucker, University of Heidelberg, IZN, Heidelberg, Germany) into pBluescript (Stratagene) generating pTau-KR with a unique *Nco*I cloning site. Next, we eliminated a unique *Spe*I site in the polylinker of pTau-KR by cutting the vector with *Spe*I, treating it with the DNA polymerase I Klenow fragment (New England Biolabs), and religating it. We created pTau-KR-linker by introducing suitable restriction sites to allow the in-frame fusion. We inserted an adapter that destroyed the *Nco*I cloning site while introducing a new *Nco*I site that was shifted by 2 bp, plus a *Spe*I and an *Eco*RV site. The primers used were TAUadapt-F (5′-TTT GGT CAT GAT GCC ATG GAC TAG TCG ATA TCT CAT GAG ATT A-3′) and TAU-link-R (5′-TAA TCT CAT GAG ATA TCG ACT AGT CCA TGG CAT CAT GAC CAA A-3′). The 1,455-nt-long coding sequence of *Mecp2* was amplified by PCR from IMAGE clone 1395411 (GenBank accession no. AI181668) and confirmed by sequencing. The PCR primers introduced a modified Kozak sequence including an *Nco*I site (ATTCC**ATG**G was changed to CCACC**ATG**G) and restriction sites that facilitated cloning. Primer RI-MeCP2-F (5′-CGGAATTCCGCCACCATGGTAGCTGGGATGTT-AGGG-3′) added an *Eco*RI site 5′ of the sequence, and primer Xba-MeCP2-R (5′-GCTCTAGAGCTCAGCTAACTCTC-TCGGTCACG-3′) added an *Xba*I site to the 3′ end. To provide the construct with a simian virus 40 (SV40) late polyadenylation signal (SV40pA), we next cloned the *Eco*RI/*Xba*I MeCP2

Abbreviations: RTT, Rett syndrome; dpc, days postcoitum.

‡To whom correspondence shout be addressed. E-mail: jaenisch@wi.mit.edu.

fragment into the *Eco*RI/*Spe*I-digested vector pZ12-I-PL2 (Ariad). MeCP2-SV40pA was released as an *Nco*I/*Spe*I fragment and cloned into pTAU-KR-linker, creating pTAU-MeCP2pA. A neo^R-resistance selectable marker from pPGKNR was isolated using *Eco*RI and *Sal*I, and overhangs were filled in using Klenow. This blunt-ended fragment was cloned into the unique *Eco*RV site of pTAU-MeCP2pA. The targeting vector pTAU-MeCP2pAneo was confirmed by sequencing.

Generation of Mice. The targeting vector was linearized with *Sac*II and electroporated into V6.5 (129 × C57BL/6) F_1 embryonic stem (ES) cell lines. We picked 96 neomycin-resistant clones, of which 63 were analyzed by Southern blots as described (14).The 5′ external probe consisted of a 528-bp PCR fragment amplified from pHV and was located 1.5 kb upstream of the *Nco*I insertion site in exon 1. The primers were Tau5′-F (5′-GAG CTG CTG CCA TCT TCA C-3′) and Tau5′-R (5′-TTT GAT GTG TGC CCT ACA GAA-3′). The 3′ external probe consisted of a 600-bp *Bam*HI/*Eco*RI genomic fragment (15) that was located 6.1 kb downstream of the insertion site. An internal probe was used to test for additional nonhomologous insertions and consisted of a 200-bp *Pst*I fragment from the neo^R ORF (15). Eleven clones were targeted correctly, which corresponds to a targeting efficiency of 17%. Two clones were used to generate chimeras by injection into (DBA/2 × C57BL/6) F_1 blastocysts as described (16). Chimeras were mated to C57BL/6 females, and offspring were analyzed for germ-line transmission. The heterozygous knock-in strain (*Tau-Mecp2* ki/+) was maintained on a mixed background that was predominantly C57BL/6 but also contained some 129 contributed by the original ES cells used for targeting. To obtain rescued males, *Tau-Mecp2* ki/+ heterozygous males were mated to heterozygous Mecp$^{1lox/+}$ females (12) that had been backcrossed to C57BL/6. After germ-line transmission was confirmed animals were routinely genotyped by PCR. For the *tau* locus the primer set Tau138 (5′-CTG GCA GAT CTT CCC GTC TA-3′), Tau1078 (5′-TGC CTG ACA GAG TCC AGA TG-3′), and Neo1323 (5′-AGG GGA TCC GTC CTG TAA GT-3′) gave a 941-bp band for the wild-type allele and a 796-bp band for the ki allele. The *Mecp2* allele was determined using primers Nsi-5 (5′-CAC CAC AGA AGT ACT ATG ATC-3′), 2lox-3 (5′-CTA GGT AAG AGC TCT TGT TGA-3′), and Nsi-3 (5′-ATG CTG ACA AGC TTT CTT CTA-3′), which generated a 180-bp wild-type band and 300-bp band for the 1lox allele.

Immunoblot Analysis. Organs were routinely harvested and snap frozen in liquid N_2. Tissues were homogenized with a Polytron homogenizer (Biospec Products) in a lysis buffer containing 125 mM Tris and 1% SDS (pH 6.8) supplemented with a proteinase inhibitor mixture (Roche). Protein concentrations were determined with a bicinchoninic acid (BCA) protein assay kit (Pierce). Sample buffer containing bromophenol blue was added to final concentrations of 12.5% glycerol and 0.25% 2-mercaptoethanol. A total of 40 μg of protein (unless indicated otherwise) was loaded on 7.5% Tris·HCl acrylamide gels (Ready Gels, Bio-Rad), probed with an anti-MeCP2 rabbit polyclonal antibody (Upstate Biotechnology) or an anti-GAPDH rabbit polyclonal (Abcam) and visualized using the Amersham Pharmacia enhanced chemiluminescence (ECL) system.

Immunohistochemistry. Brains were harvested from 8-week-old animals, weighed, immersion-fixed for 20 h in 10% phosphate buffered formalin, and cryoprotected for 24 to 36 h in 30% sucrose and embedded in OCT. A series of 15-μm sagittal sections were slide mounted and stored at −20°C. For immunohistochemistry, slides were blocked in 5% normal goat serum and incubated with rabbit antibody raised against the C-terminal peptide of MeCP2 (11) at a dilution of 1:500 and a mouse antineuron-specific nuclear protein (NeuN, Chemicon) at a dilution of 1:200. The MeCP2 antibody was detected with a FITC-conjugated goat anti-rabbit IgG and the NeuN antibody with a Rhodamine-conjugated donkey anti-mouse IgG (both from Jackson ImmunoResearch), both at a dilution of 1:500. Sections were finally rinsed in PBS/DAPI (4′,6-diamidino-2-phenylindole, 1:10,000) and mounted in Vectashield (Vector laboratories). Images were taken with a Leica fluorescence microscope under ×20 magnification.

RNA Samples and RNase Protection Assay. Embryo heads and adult brains were harvested, snap frozen in liquid N_2, and subsequently extracted with RNA-Bee (Tel-Test, Friendswood, TX). Embryos were isolated from *Tau-Mecp2* ki/+ females mated with *Tau-Mecp2* ki/+ males. Embryos of the correct genotype were identified by PCR genotyping using DNA extracted from embryos (10.5–15.5 days postcoitum, dpc), yolk sac (9.75 dpc), or tail tips.

For the RNase protection assay, the probe template was generated by PCR from genomic DNA obtained from a transgenic mouse with primers TauExon1–27F (5′-GCCAGGAGTTTGACACAATG-3′) and MeCP2–282R (5′-CATACATAGGTCCCCGGTCA-3′). The PCR product was cloned into the vector pCR2.1-TOPO (TOPO TA Cloning kit, Invitrogen) and subcloned as a *Pst*I fragment into the transcription vector pSP72 (Promega). *In vitro* transcription was carried out with the Maxiscript T7 Kit (Ambion, Austin, TX). UTPαP^{32} (3,000 Ci/mmol, 10 mCi/ml, Amersham Biosciences, 1 Ci = 37 GBq) was diluted 1:10 with unlabeled nucleotide, and the probes were gel-purified. A total of 2,000 cpm of probe and 10 μg of total RNA was used in the assay according to the manufacturer's specification (Ambion RPA III kit). The samples were resolved on a 6% acrylamide gel (1:30 bisacrylamide) and quantified by PhosphorImaging.

Spontaneous Activity Measurements. Motor activity was measured using an infrared beam-activated movement-monitoring chamber (Opto-Varimax-MiniA, Columbus Instruments). For each experiment, a mouse was placed in the chamber at least 3 h before recordings started. Movement was monitored during the normal 12-h dark cycle (7 p.m. to 7 a.m.).

Results

Expression of MeCP2 from the *tau* Locus. To express MeCP2 specifically in postmitotic neurons, we designed a targeting construct that places *Mecp2* expression under the control of the promoter of the microtubule-binding protein, Tau. Tau protein is strongly expressed in neurons (17), and the endogenous *tau* locus has been used previously to drive neuron-specific expression of enhanced GFP (EGFP) (15). Homozygous animals mutant for *tau* have been shown to be phenotypically indistinguishable from wild-type littermates (18). A cDNA containing the *Mecp2* coding sequence, including a modified Kozak sequence (19), was placed into exon 1 of the *tau* gene in-frame with the endogenous initiation codon thereby creating a fusion protein that contains the first 31 amino acids of Tau (Tau-MeCP2, Fig. 1*A*). The targeting construct was introduced into V6.5 embryonic stem cells by electroporation, and 63 neomycin-resistant clones were analyzed. Eleven clones were targeted correctly, and two of these (Fig. 1*B*) were used to generate germ-line-transmitting chimeras.

To examine and compare the expression pattern of Tau-MeCP2 and endogenous MeCP2, we determined their protein levels in various adult mouse tissues by immunoblot analysis (Fig. 2 *A* and *B*). We found that Tau-MeCP2 expression in the brain was 2- to 4-fold higher than endogenous MeCP2 (Fig. 2*A*, lanes 4–9). Endogenous MeCP2 was expressed highly in lung and spleen, and moderately in kidney and heart and liver (Fig. 2*B*, wt). Tau-MeCP2 protein expression was high in lung and kidney,

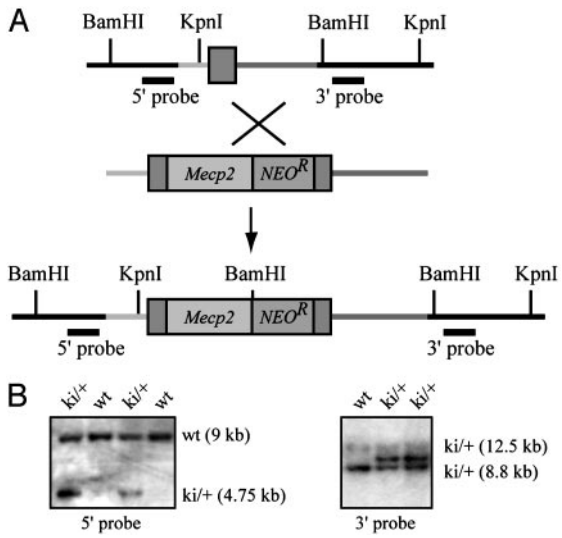

Fig. 1. Targeting the MeCP2 cDNA to the tau locus. (*A*) Targeting strategy to insert the *Mecp2* cDNA and the neomycin resistance marker (*NEO*^{R}) into exon 1 of the *tau* locus. The upstream and downstream targeting arms are shown in light and dark gray, respectively. The locations of 5′ and 3′ external probes used for Southern blot analysis are indicated. (*B*) Southern blot analysis of targeted embryonic stem cell clones (ki/+) after digestion with *Bam*HI (*Left*) and *Kpn*I (*Right*). When hybridized with the 5′ external probe, wild-type clones display a 9-kb band. The correct targeting event results in a band-shift to 4.75 kb for the targeted allele. Hybridization with the 3′ external probe results in a 8.8-kb wild-type band and a 12.5-kb band for the targeted allele.

and was low in heart (Fig. 2 *B* and *R*). Very low expression in liver and spleen was detectable after long exposure times.

MeCP2 localizes to highly methylated centromeric heterochromatin (20), and immunohistochemical analysis revealed the typical punctate nuclear MeCP2 staining pattern in wild-type brains (Fig. 2*C*). This pattern was not detectable in *Mecp2* mutant animals. Instead, a faint diffuse nuclear staining was observed, which probably arose from the detection of the truncated MeCP2 protein (Fig. 2*G*) (12). The deletion of exon 3 encompasses most of the methyl-CpG-binding domain (MBD), but the C-terminal epitope including the nuclear localization sequence (NLS) remains largely intact (12). We found that, in *Mecp2* mutant mice heterozygous for the *Tau-Mecp2* transgene (rescued animals), MeCP2 distribution was indistinguishable from wild-type MeCP2 (Fig. 2*K*), suggesting correct localization of the fusion protein. This was to be expected, because the MBD and the NLS have both been shown to be necessary and possibly sufficient for the specific localization of MeCP2 (20). The axonal localization signal of Tau is located in the 3′ UTR, and therefore is not part of the Tau-MeCP2 mRNA (21). In addition, we found that all MeCP2-positive cells were double labeled with an antibody against the neuron-specific marker protein NeuN (22) (Fig. 2 *E*, *M*, and *Q*), indicating that endogenous MeCP2 as well as Tau-MeCP2 were detectable only in neuronal cells (Fig. 2 *F*, *N*, and *R*).

Timing of Tau-MeCP2 Expression. To quantify the relative expression of *Mecp2* and *Tau-Mecp2* during embryonic development, we carried out an RNase protection assay (RPA) on embryos harvested between 9.75 and 15.5 dpc. The probe (RPA) was designed to span the *Tau-Mecp2* junction including 82 bp of *tau* exon 1 and 164 bp of the *Mecp2* cDNA. This allowed the detection of the *Tau-Mecp2* RNA as well as the endogenous *Mecp2* and *tau* transcripts (Fig. 3*A*). *Mecp2* RNA was detectable as early as 9.75 dpc with levels steadily increasing until they reached adult levels at 15.5 dpc (Fig. 3*B*, compare lane 5 with lanes 6 and 9). *Tau-Mecp2* expression followed closely that of endogenous *tau*, with RNA being present starting at 10.5 dpc and, like *Mecp2*, reaching maximum expression levels at 15.5 dpc (Fig. 3*B*, compare lane 5 with lanes 6 and 9). The timing of *Tau-Mecp2* expression therefore appeared to closely mimic that of *Mecp2*.

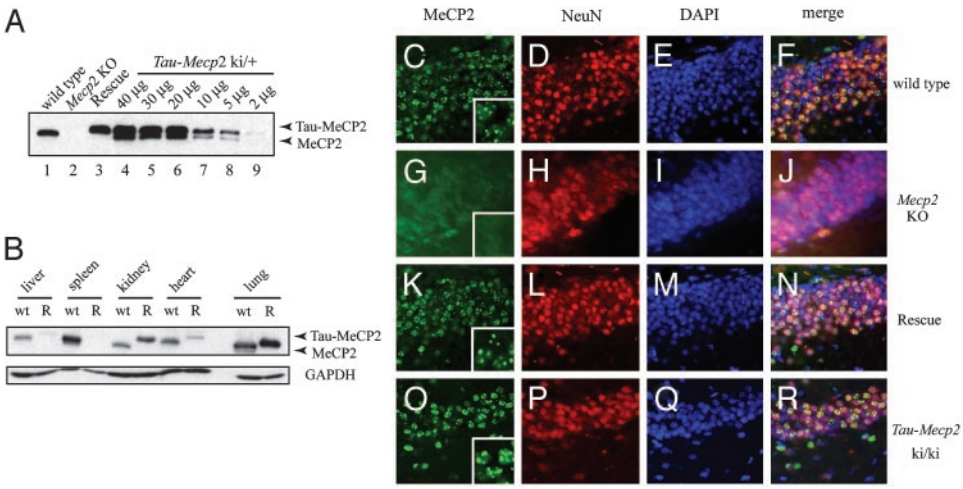

Fig. 2. Expression of MeCP2 from the *tau* locus. (*A*) Immunoblot analysis of protein prepared from whole brain samples. As controls, 40 μg of protein were loaded from wild-type and *Mecp2* mutant (*Mecp2* KO) animals, and *Mecp2* mutant animals heterozygous for the *Tau-Mecp2* transgene (Rescue). The protein extract from a *Mecp2* wild-type animal heterozygous for the transgene (*Tau-Mecp2* ki/+) was loaded as serial dilutions as indicated. The Tau-MeCP2 fusion protein contains 31 aa of the Tau protein, which results in a band shift. (*B*) Endogenous MeCP2 (wild-type animal, wt) is highly expressed in the lung and spleen, and less in the liver, kidney, and heart. Tau-MeCP2 expression (rescued animal, R) is high in lung and kidney. Low-level expression is also detectable in the heart. In the liver and spleen Tau-MeCP2 is detectable only after long exposure times. (*C–R*) Tau-MeCP2 expression is neuron-specific in the brain and localizes to heterochromatic foci. Double labeled immuno-fluorescence of MeCP2 (green) and neuron-specific nuclear protein (NeuN, red) from wild-type (*C–F*), *Mecp2* KO (*G–J*), rescued (*K–N*) and *Tau-Mecp2* homozygous (*Tau-Mecp2* ki/ki, *O–R*) hippocampi of adult animals are shown. Punctate MeCP2 staining is detectable in wild-type animals (*C*) as well as animals carrying the *Tau-Mecp2* transgene (*K* and *O*). *Insets* in *C*, *G*, *K*, and *O* show enlargements of a small number of cells to illustrate MeCP2 staining. Endogenous MeCP2 as well as Tau-MeCP2 expression overlaps with NeuN immunoreactivity (*F*, *N*, and *R*). Only weak diffuse MeCP2 staining is present in *Mecp2* null cells (*G*). Nuclear 4′,6-diamidino-2-phenylindole (DAPI) stain is shown in blue (*E*, *I*, *M*, and *Q*).

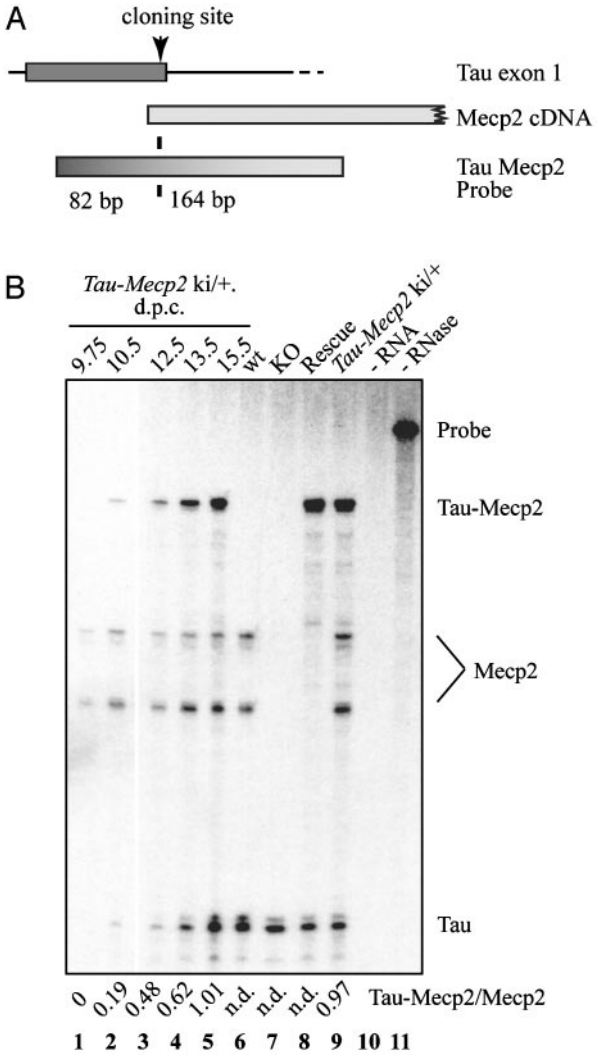

Fig. 3. Timing of *Tau-Mecp2* expression. (*A*) Probe design for the RNase protection assay. The probe overlaps the *Tau-Mecp2* junction of the transgene and consists of 82 bp of *Tau* sequence and 164 bp of *Mecp2* cDNA sequence (26 bp of exon 2 and 138 bp of exon 3). (*B*) RNase protection assay. RNA was extracted from embryos (9.75 dpc) and embryonic heads (10.5–15.5 dpc) of *Mecp2* wild-type animals heterozygous for the *Tau-Mecp2* transgene (lanes 1–5), or from brains of adult control animals (lanes 6–9). Lane 10 shows the no sample control, and lane 11 is 15% loading of the no RNase control. Wild-type *Mecp2* RNA is detectable as two bands that probably represent different splice products (lanes 1–6 and 9). No *Mecp2* signal is detectable in animals carrying the mutant *Mecp2* allele that lacks exon 3 (lanes 7 and 8). The ratio of *Tau-Mecp2* RNA expression to endogenous *Mecp2* RNA as quantitated by phosphorimaging is given below the gel.

Quantification of expression levels revealed that, in 15.5 dpc embryonic heads as well as in adult brains, the amount of *Mecp2* RNA appeared to be similar to *Tau-Mecp2* RNA. On the protein level, however, Tau-MeCP2 was two to four times more abundant (Fig. 2*A*), suggesting a difference in either translation efficiency of the transcripts or protein stability.

Overexpression of MeCP2 Is Detrimental. Wild-type animals heterozygous for the transgene were fertile and healthy with no obvious phenotypic abnormalities. In contrast, wild-type as well as *Mecp2* mutant animals homozygous for the transgene suffered from profound motor dysfunction including side-to-side swaying, tremors, and gait ataxia. There was no reduction in brain weight in animals at 2–4 months of age (data not shown). Animals were of normal weight at birth, but by weaning age pups were severely runted and up to 60% smaller than wild-type littermates (Fig. 4*B*). The condition improved when animals were fostered in small groups, indicating that the failure to thrive was largely caused by their inability to compete with littermates for food. Once the animals reached weaning age, the phenotype appeared to be stable, but they remained small and did not mate. By 9 months, ataxia and tremors appeared to have intensified. The animals were emaciated, had a disheveled look, and developed additional problems such as cataracts and lesions. The lesions were probably caused by excessive stereotypic scratching. However, no premature death was observed. Preliminary data suggest that *Mecp2*-mutant animals homozygous for the transgene were slightly less affected compared to *Mecp2* wild-type animals homozygous for the transgene as judged by weight and appearance (data not shown). The phenotype was specific and not caused by the lack of Tau protein because animals homozygous for other transgenes targeted to exon 1 of the *tau* locus were phenotypically normal (ref. 15 and unpublished data).

Immunohistochemical analysis of brain sections revealed a punctate MeCP2 staining pattern (Fig. 2*M*), suggesting that the level of Tau-MeCP2 overexpression had no effect on Tau-MeCP2 localization in adult mice. Previous reports detected diffuse nuclear MeCP2 staining at 10 dpc, which became increasingly punctate through 16.5 dpc (5). Our results suggest that MeCP2 dosage is critical and that overexpression of MeCP2 4- to 6-fold above wild-type level is detrimental to the health of the animal.

Expression of MeCP2 in Postmitotic Neurons Rescues the RTT Phenotype. *Mecp2* mutant mice die, on average, at ≈10 weeks of age (12). In contrast, mutant animals heterozygous for the transgene were healthy and fertile and, in various crosses, passed on all alleles at the expected Mendelian ratios (data not shown). They were phenotypically indistinguishable from their wild-type littermates and displayed no RTT-like symptoms (Fig. 4*A*). A distinct feature of *Mecp2* mutant animals are weight abnormalities, and in agreement with previous reports (13), *Mecp2* mutant animals were severely underweight from 4–5 weeks of age (Fig. 4*C*). In contrast, the weight of rescued animals was indistinguishable from that of wild-type littermates throughout postnatal development (Fig. 4*C*).

Human RTT syndrome, as well as the *Mecp2* mutant mouse phenotype, is characterized by a decrease in head growth and neuronal cell size as well as increased cell packing density throughout the brain (12, 23–25). As published previously, we found a 14–18% reduction in brain weight in 8- to 13-week-old *Mecp2* mutant animals. In contrast, rescued animals showed no difference in brain weight compared to wild-type littermates, even when brains were harvested as late as 5 months of age (Fig. 4*D*). Hypoactivity is another characteristic of *Mecp2* mutant mice (12, 13, 26). We tested exploratory response as well as total nocturnal activity by placing animals in cages equipped with an infrared beam movement detector. The age of the mice tested ranged from 4 to 6.5 months, long after the onset of RTT symptoms in *Mecp2* mutant mice and in all cases after *Mecp2* mutant littermates had died. In both behavioral tests, rescued animals were indistinguishable from wild-type littermates (Fig. 4*E*).

In summary, our data indicate that rescued animals do not display any of the common RTT phenotypes that have been described for *Mecp2* mutant animals. Therefore, expression of *Mecp2* in postmitotic neurons is sufficient to alleviate the RTT phenotype, even at slightly elevated protein levels.

Discussion

Mutation of the methyl-binding protein MeCP2 leads to RTT in humans, and increasing evidence suggests that this disorder is

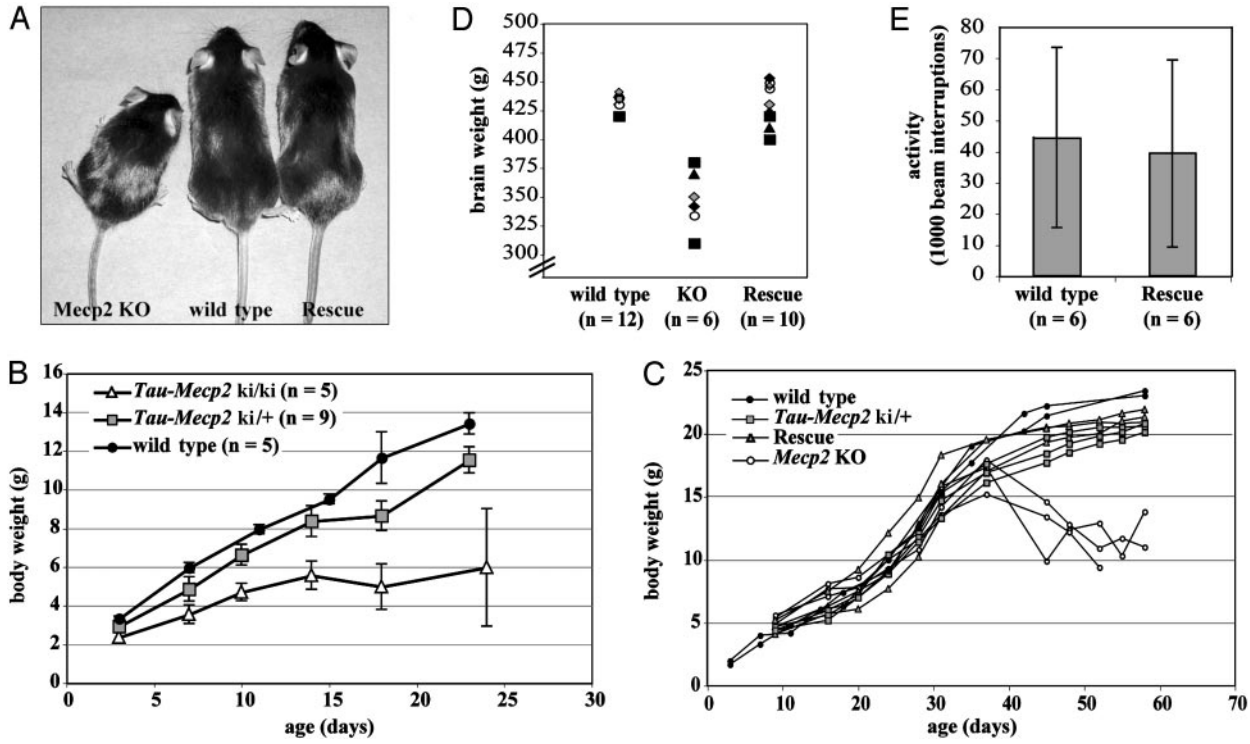

Fig. 4. Expression of MeCP2 in postmitotic neurons rescues the RTT phenotype, but overexpression of MeCP2 is detrimental. (*A*) Rescued animals are indistinguishable from their wild-type littermates. Animals are shown at 8 weeks of age. (*B*) *Mecp2* wild-type animals heterozygous for *Tau-Mecp2* (*Tau-Mecp2* ki/+) show normal physical development. *Mecp2* overexpressing animals (*Tau-Mecp2* ki/ki) have a normal birth weight, but progressively lose weight so that animals are up to 60% smaller than wild-type littermates at weaning age. (*C*) Neuronal expression of MeCP2 rescues the weight-loss phenotype. *Mecp2* null animals start to lose weight at ≈5 weeks of age. The weight of rescued as well as *Tau-Mecp2* ki/+ animals is comparable to that of wild-type littermates. (*D*) Rescued animals have a brain weight comparable to wild-type littermates. In contrast, *Mecp2* mutant animals show a 15–18% reduction in brain weight. (*E*) Spontaneous activity of rescued animals is comparable with the activity of wild-type littermates as measured by an infrared beam activated movement detector.

primarily caused by a defect in neuronal maintenance and maturation. In a mouse model, loss of MeCP2 expression leads to a RTT-like phenotype including tremors, heavy breathing, hypoactivity, and smaller brain size associated with smaller, more densely packed neurons. After the onset of symptoms at 4 to 6 weeks of age and progressive physical deterioration, the animals typically die at ≈10–12 weeks of age (12, 13). Deletion of *Mecp2* exon 3, encoding most of the methyl-binding domain in neural progenitor cells, produces a phenotype that is indistinguishable from the germ-line mutation. In contrast, loss of MeCP2 function in postmitotic neurons of the postnatal brain led to a delayed onset of symptoms by up to 3 months (12). MeCP2 is primarily expressed in mature neuronal populations (5–7) with an expression pattern that follows the maturation of the CNS (5). Recent studies suggest that MeCP2 may be important for the maintenance and modulation of synapses (9). In addition, neurons of RTT individuals appear to show a reduction in dendritic complexity (27). Also, recent experiments in *Xenopus* revealed a specific function of MeCP2 in early neural development (28).

Here we provide functional evidence for the requirement of MeCP2 in postmitotic neurons by placing the *Mecp2* cDNA under the control of the endogenous promoter of the microtubule-binding protein, Tau. By introducing the cDNA into exon 1 of the *tau* gene in-frame with the endogenous start codon, we created a fusion protein that contained the first 31 amino acids of Tau (Tau-MeCP2). Tau-MeCP2 was expressed at a level 2- to 4-fold higher than endogenous MeCP2, and the onset of expression correlated closely with endogenous *tau* expression being first detectable at 10.5 dpc. In agreement with previous reports, endogenous *Mecp2* RNA was detectable at 9.75 dpc. Immunohistochemical analysis of brain sections revealed that Tau-MeCP2 localized like endogenous MeCP2 to heterochromatic foci of postmitotic neurons in adult mice.

One copy of the *Tau-Mecp2* transgene led to the complete rescue of all assessed phenotypes in *Mecp2* mutant animals. They had a normal lifespan and showed normal physical development as judged by weight. The rescued animals had normal brain weight and showed no signs of hypoactivity, tremors, or any other physical symptoms typically associated with RTT, even at an advanced age of 6 months or more. We therefore conclude that expression of MeCP2 in postmitotic neurons is sufficient to alleviate the phenotype in MeCP2 mutant mice. Our data strongly suggest that the RTT phenotype is caused by lack of MeCP2 in the brain. Nevertheless, we cannot fully exclude a contribution of MeCP2 in some peripheral tissues, because the physiological basis of some symptoms in RTT patients as well as in *Mecp2* mutant animals still remains to be determined.

It has been reported that there is no obvious correlation between MeCP2 protein and RNA levels in adult tissues, suggesting that *Mecp2* translation may be postranscriptionally regulated (5). The endogenous *Mecp2* sequence contains a 182-bp 5′ UTR and a highly conserved 8.5-kb 3′ UTR with alternative polyadenylation (pA) signals. Depending on which pA signal is used, either a 1.9-kb or a 10-kb transcript is produced. In the brain, the 10-kb transcript is the predominant one (29). In our experiments, the *Tau-Mecp2* construct did not include either of the untranslated regions. Because both the short and the long transcript have similar half-lives (29), it is possible that the 3′ UTR contains regulatory elements important for translation efficiency. In fact, the *Mecp2* 3′ UTR has recently been predicted

to contain potential target sequences for microRNAs, which confer posttranslational repression (30).

Moderate overexpression of MeCP2 in wild-type mice heterozygous for *Tau-Mecp2* had no adverse effect. In contrast, homozygosity for the transgene led to severe motor dysfunction in a wild-type as well as a *Mecp2* mutant background. The result was an impaired ability to compete with littermates for food, leaving the pups severely runted. Symptoms included tremors, gait ataxia, and side-to side swaying. These observations suggest that neurons can tolerate a 2- to 3-fold higher level of MeCP2 expression but that higher expression levels result in obvious detrimental consequences. Interestingly, *Mecp2* mutant animals homozygous for the transgene showed a slightly less severe phenotype, which emphasizes the importance of MeCP2 dosage.

We found that MeCP2 expression was dispensable through early embryonic development. In agreement with this finding, previous studies described that MeCP2 expression was undetectable before 9.5 dpc on the RNA or protein level, indicating that it plays no essential role in early embryonic development (5, 31). Moreover, we find that MeCP2 is not necessary for neurogenesis, despite the fact that MeCP2 appears to be expressed in some neuronal precursor cells of the rodent brain (32). The delayed phenotype of the conditional mutant observed after postnatal loss of MeCP2 function in postmitotic neurons may be attributable to the fact that the expression of CamKII-driven Cre recombinase used in this experiment is limited to certain parts of the postnatal brain, including the forebrain, hippocampus, and brainstem. It is only marginally active in the cerebellum, a region where *Mecp2* mRNA is highly expressed (32). In contrast, loss of MeCP2 function in neural progenitor cells affects essentially all neurons. It is also possible that the abatement of the phenotype of CamKII-Cre mutants is caused by the presence of MeCP2 in neurons during prenatal development or the lack of Cre expression in a crucial cell type.

Our results are consistent with MeCP2 playing no essential role in the early stages of brain development. It is possible, in fact, that neurons are functionally normal in the young postnatal patient, and that neural dysfunction becomes manifest only later because of prolonged MeCP2 deficiency. If correct, therapeutic strategies could be aimed at preventing postnatal dysfunctions from developing in *MECP2* mutant neurons.

We thank members of the Jaenisch lab for discussions and critical comments on the manuscript. We also thank K. Tucker for providing reagents, J. Dausman for blastocyst injections, R. Flannery for animal care, and A. Caron (MIT Center for Cancer Research histology facility) for technical support. This work was conducted using the W. M. Keck biological imaging facility at the Whitehead Institute and was supported by National Institutes of Health Grant CA87869 (to R.J.) and the Rett Syndrome Research Foundation.

1. Zoghbi, H. Y. (2003) *Science* **302,** 826–830.
2. Kriaucionis, S. & Bird, A. (2003) *Hum. Mol. Genet.* **12,** Spec. No. 2, R221–R227.
3. Amir, R. E., Van den Veyver, I. B., Wan, M., Tran, C. Q., Francke, U. & Zoghbi, H. Y. (1999) *Nat. Genet.* **23,** 185–188.
4. Nan, X., Ng, H. H., Johnson, C. A., Laherty, C. D., Turner, B. M., Eisenman, R. N. & Bird, A. (1998) *Nature* **393,** 386–389.
5. Shahbazian, M. D., Antalffy, B., Armstrong, D. L. & Zoghbi, H. Y. (2002) *Hum. Mol. Genet.* **11,** 115–124.
6. Akbarian, S., Chen, R. Z., Gribnau, J., Rasmussen, T. P., Fong, H., Jaenisch, R. & Jones, E. G. (2001) *Neurobiol. Dis.* **8,** 784–791.
7. Coy, J. F., Sedlacek, Z., Bachner, D., Delius, H. & Poustka, A. (1999) *Hum. Mol. Genet.* **8,** 1253–1262.
8. Mullaney, B. C., Johnston, M. V. & Blue, M. E. (2004) *Neuroscience* **123,** 939–949.
9. Cohen, D. R., Matarazzo, V., Palmer, A. M., Tu, Y., Jeon, O. H., Pevsner, J. & Ronnett, G. V. (2003) *Mol. Cell. Neurosci.* **22,** 417–429.
10. Tudor, M., Akbarian, S., Chen, R. Z. & Jaenisch, R. (2002) *Proc. Natl. Acad. Sci. USA* **99,** 15536–15541.
11. Chen, W. G., Chang, Q., Lin, Y., Meissner, A., West, A. E., Griffith, E. C., Jaenisch, R. & Greenberg, M. E. (2003) *Science* **302,** 885–889.
12. Chen, R. Z., Akbarian, S., Tudor, M. & Jaenisch, R. (2001) *Nat. Genet.* **27,** 327–331.
13. Guy, J., Hendrich, B., Holmes, M., Martin, J. E. & Bird, A. (2001) *Nat. Genet.* **27,** 322–326.
14. Sambrook, J., Fritsch, E. F. & Maniatis, T. (1989) *Molecular Cloning: A Laboratory Manual* (Cold Spring Harbor Lab. Press, Plainview, NY).
15. Tucker, K. L., Meyer, M. & Barde, Y. A. (2001) *Nat. Neurosci.* **4,** 29–37.
16. Hogan, B., Beddington, R., Costantini, F. & Laciy, E. (1994) *Manipulating the Mouse Embryo: A Laboratory Manual* (Cold Spring Harbor Lab. Press, Plainview, NY).
17. Binder, L. I., Frankfurter, A. & Rebhun, L. I. (1985) *J. Cell Biol.* **101,** 1371–1378.
18. Harada, A., Oguchi, K., Okabe, S., Kuno, J., Terada, S., Ohshima, T., Sato-Yoshitake, R., Takei, Y., Noda, T. & Hirokawa, N. (1994) *Nature* **369,** 488–491.
19. Kozak, M. (1986) *Cell* **44,** 283–292.
20. Nan, X., Tate, P., Li, E. & Bird, A. (1996) *Mol. Cell. Biol.* **16,** 414–421.
21. Aronov, S., Aranda, G., Behar, L. & Ginzburg, I. (2001) *J. Neurosci.* **21,** 6577–6587.
22. Mullen, R. J., Buck, C. R. & Smith, A. M. (1992) *Development (Cambridge, U.K.)* **116,** 201–211.
23. Jellinger, K., Armstrong, D., Zoghbi, H. Y. & Percy, A. K. (1988) *Acta Neuropathol.* **76,** 142–158.
24. Hagberg, G., Stenbom, Y. & Engerstrom, I. W. (2001) *Brain Dev.* **23,** Suppl. 1, S227–S229.
25. Bauman, M. L., Kemper, T. L. & Arin, D. M. (1995) *Neuropediatrics* **26,** 105–108.
26. Shahbazian, M., Young, J., Yuva-Paylor, L., Spencer, C., Antalffy, B., Noebels, J., Armstrong, D., Paylor, R. & Zoghbi, H. (2002) *Neuron* **35,** 243–254.
27. Armstrong, D., Dunn, J. K., Antalffy, B. & Trivedi, R. (1995) *J. Neuropathol. Exp. Neurol.* **54,** 195–201.
28. Stancheva, I., Collins, A. L., Van den Veyver, I. B., Zoghbi, H. & Meehan, R. R. (2003) *Mol. Cell* **12,** 425–435.
29. Reichwald, K., Thiesen, J., Wiehe, T., Weitzel, J., Poustka, W. A., Rosenthal, A., Platzer, M., Stratling, W. H. & Kioschis, P. (2000) *Mamm. Genome* **11,** 182–190.
30. Lewis, B. P., Shih, I. H., Jones-Rhoades, M. W., Bartel, D. P. & Burge, C. B. (2003) *Cell* **115,** 787–798.
31. Kantor, B., Makedonski, K., Shemer, R. & Razin, A. (2003) *Gene Exp. Patterns* **3,** 697–702.
32. Jung, B. P., Jugloff, D. G., Zhang, G., Logan, R., Brown, S. & Eubanks, J. H. (2003) *J. Neurobiol.* **55,** 86–96.